Title

Plastic Deformation of Polymer Blends as a Means to Achieve Stretchable Organic Transistors

Journal

Advanced Electronic Materials, 3(1)

ISSN

2199-160X

Authors

Sun, Tianlei
Scott, Joshua I
Wang, Ming
et al.

Publication Date

2017

DOI

10.1002/aelm.201600388

Peer reviewed

Published in final edited form as:

Adv Electron Mater. 2017 January ; 3(1): . doi:10.1002/aelm.201600388.

Reversible Plastic Deformation of Polymer Blends as a Means to Achieve Stretchable Organic Transistors

Tianlei Sun,
Department of Mechanical and Aerospace Engineering, North Carolina State University, Raleigh, NC 27695, USA

Joshua I. Scott,
Department of Mechanical and Aerospace Engineering, North Carolina State University, Raleigh, NC 27695, USA

Ming Wang, Dr.,
Center for Polymers and Organic Solids, University of California-Santa Barbara, Santa Barbara, CA 93106, USA

R. Joseph Kline, Dr.,
National Institute of Standards and Technology, Gaithersburg MD, 20899, USA

Guillermo Bazan, Dr., and
Center for Polymers and Organic Solids, University of California-Santa Barbara, Santa Barbara, CA 93106, USA

Brendan T. O'Connor, Dr.
Department of Mechanical and Aerospace Engineering, North Carolina State University, Raleigh, NC 27695, USA

Abstract

Intrinsically stretchable semiconductors will facilitate the realization of seamlessly integrated stretchable electronics. However, to date demonstrations of intrinsically stretchable semiconductors have been limited. In this study, a new approach to achieve intrinsically stretchable semiconductors is introduced by blending a rigid high-performance donor-acceptor polymer semiconductor poly[4(4,4dihexadecyl4Hcyclopenta [1,2b:5,4b'] dithiopen2yl) alt [1,2,5] thiadiazolo [3,4c] pyridine] (PCDTPT) with a ductile polymer semiconductor poly(3hexylthiophene) (P3HT). Under large tensile strains of up to 75%, the polymers are shown to orient in the direction of strain, and when the strain is reduced, the polymers reversibly deform. During cyclic strain, the local packing order of the polymers is shown to be remarkably stable. The saturated field effect charge mobility is shown to be consistently above 0.04 $cm^2 V^{-1}s^{-1}$ for up to 100 strain cycles with strain ranging from 10% to 75% when the film is printed onto a rigid test bed. At the 75% strain state, the charge mobility is consistently above 0.15 $cm^2 V^{-1}s^{-1}$. Ultimately, the polymer blend process introduced here results in an excellent combination of device

Correspondence to: Brendan T. O'Connor.

Supporting Information: Supporting Information is available from the Wiley Online Library or from the author.

performance and stretchability providing an effective approach to achieve intrinsically stretchable semiconductors.

Graphical abstract

A high performance intrinsically stretchable semiconductor is demonstrated based on a polymer blend of a high performance polymer semiconductor PCDTPT and a ductile polymer semiconductor P3HT. The film is shown to plastically deform in tension and compression with very stable local polymer order resulting in stable charge mobility. This is the first demonstration of a stretchable semiconductor composed solely of polymer semiconductors.

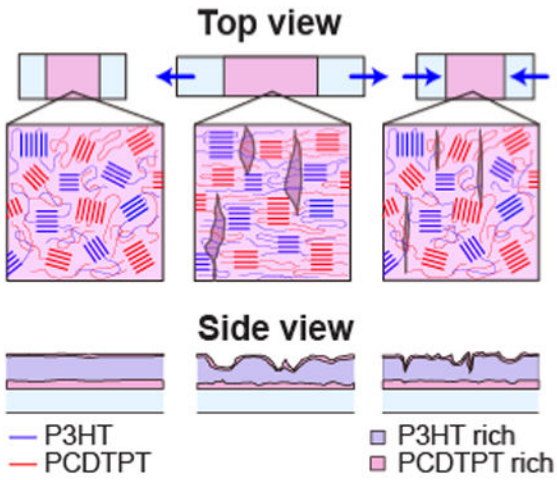

Keywords

polymer semiconductors; blend films; stretchable electronics; morphology; organic transistors

1. Introduction

Electronics that are able to maintain their function during large deformation provide opportunities for integration into a range of transformative technologies, from soft-robotics to bio-integrated devices.[1, 2] This vision has resulted in a growing number of demonstrations of stretchable electronic devices including photovoltaics,[3, 4] light emitting devices,[5, 6] sensors[1, 7] and transistors.[8-10] To impart the ability for devices to reversibly stretch, approaches include the use of geometric structures that minimize strain on the active components,[2, 3, 11] and employing intrinsically stretchable materials.[10, 12, 13] The development of intrinsically stretchable devices is particularly attractive due the ability to achieve larger device densities, greater strain limits, and seamless integration into stretchable applications. In order to achieve an intrinsically stretchable device, all the layers composing the device need to be stretchable.[8, 10] A particular challenge in realizing these devices is the development of intrinsically stretchable semiconductor layers.[10] In the search of stretchable semiconductors, polymers are an attractive material system to explore given the ability to manipulate their plasticity, and the long history in the development of polymers with large reversible elasticity (i.e. elastomers).[14] Examples of intrinsically stretchable

polymer semiconductors include the demonstration of a tri-block co-polymer based on poly(3-hexylthiophene) (P3HT) and poly(methyl methacrylate) (PMMA) to form a thermoplastic elastomer that was able to stretch by 140%.[13] However, the field effect mobility was limited to approximately 10^{-4} $cm^{-2}V^{-1}s^{-1}$. More recently, a cross-linked diketopyrrolopyrrole (DPP) polymer was synthesized with a consistent field effect mobility above 0.4 $cm^2V^{-1}s^{-1}$ over a strain range of 20%.[15] Another approach has been to form a fibril network of polymer semiconductor material embedded into an elastomer host.[16-18] However, this approach consists of a sparse network of semiconductor material that may limit performance, and can still result in fibril fracture at large strain. An alternative approach is to modify the plasticity of the polymer of interest. There have been a number of reports on changing the plasticity of electrically conducting polymer films through modification of the molecular structure,[19, 20] morphology,[20, 21] and through the use of additives.[22-26] While these approaches have shown a change in plasticity, there have been limited reports on repeated stretchability of the films. Recently, the conductive polymer PEDOT:PSS was shown to be highly deformable when incorporating the plasticizer Triton X-100,[24] which was attributed to lowering the glass transition temperature (T_g) of the film. However, there have not been demonstrations of plasticizers used in polymer semiconductors to achieve stretchable films, likely due to the added disorder and packing density caused by the additives and a subsequent reduction in charge mobility.[10] Here, we introduce a novel approach to achieve intrinsically stretchable polymer semiconductors. We employ a polymer semiconductor blend film that is shown to plastically deform in tension and compression when on an elastomer substrate allowing for a highly deformable organic semiconductor with high charge mobility when applied in an organic thin film transistor (OTFT). Previously, blending polymer semiconductors has been shown to modify the mechanical response of the film while maintaining charge transport behavior.[25, 27] While the ductility of films were shown to increase, the ability to cyclically stretch while maintaining electrical properties has not been shown. For a semiconductor that will be used in stretchable devices, not only is it important to be able to survive large tensile strain, but to also function after the reduction of the applied strain. Here, we achieve this cyclic strain capability by blending a high performance polymer poly[4-(4,4-dihexadecyl-4H-cyclopenta[1,2-b:5,4-b,]dithiophen-2-yl)-alt-[1,2,5]thiadiazolo[3,4-c]pyridine] (PCDTPT)[28] with a highly ductile polymer P3HT. PCDTPT has been shown to be a high performance polymer semiconductor when applied in an OTFT, but is relatively brittle and cracks at a few percent strain.[25] Blending P3HT with PCDTPT significantly increases the ductility of the film over neat PCDTPT; while also maintaining the charge mobility associated with the higher performing PCDTPT when applied in an OTFT. This behavior was attributed to vertical segregation of the PCDTPT toward the gate dielectric interface, while also having significant intermixing of both polymers throughout the films thickness, as illustrated in Figure 1.[25] In this work, we explore the ability of P3HT:PCDTPT blend films to function well under large cyclic strain. The morphology and charge transport is characterized for the film strained by 75% and released back to 10% strain, relative to its original length under a specified number of cycles. We show that the films can be cyclically strained up to 100 times while showing stable charge transport behavior owing primarily to the reversible plastic deformation behavior of the blend film with highly stable local polymer order. This represents a novel approach to achieve intrinsically stretchable

semiconductor consisting solely of semiconductor materials. Below we first discuss the morphology of the blend film under cyclic strain followed by charge transport characterization.

2. Results and Discussion

Films were first spun cast onto octyltrichlorosilane (OTS) treated silicon and then transfer printed to a polydimethylsiloxane (PDMS) elastomer substrate. The film-PDMS stack was then elongated in tension to a specified strain. For cyclic strain, the film-PDMS stack was strained to 75% and then strain was released back to 10% relative to its unstrained state, and repeated for a specified number of cycles. After the strain process was complete, the films were either characterized while on the PDMS substrate, or transfer printed onto a secondary substrate for further characterization. Images of a film being strained is shown in Figure 1 along with a schematic of the cyclic strain process, and the lamination onto a transistor test bed for charge transport characterization. Our previous report investigating PCDTPT:P3HT blend films showed that the blend ratio had a significant impact on the segregation characteristics and ductility of the film.[25] A 1:1 PCDTPT:P3HT blend ratio by weight had a charge mobility similar to the neat PCDTPT film, but in addition to vertical segregation, large lateral segregation of the PCDTPT was observed that limited the crack onset strain to under 50%. When reducing the ratio to 1:4 the lateral segregation was suppressed and ductility increased but there was a decrease in charge mobility. Here we focus on a polymer ratio of 4:6 by weight; approaching the 1:1 ratio to maximize charge mobility but without gross lateral segregation of the PCDTPT, resulting in highly ductile films, as we show below. An optimization of the blend film was not performed, and further optimization of the polymer ratio and processing conditions may lead to further performance gains.

2.1. Film Morphology

The change in morphology under large cyclic strain is first characterized by measuring the films with UV-visible spectroscopy under linearly polarized light while the film was on a PDMS substrate. P3HT and PCDTPT absorb light over different spectral ranges of approximately 400 nm to 620 nm for P3HT and 650 nm to 1100 nm for PCDTPT, as shown in Figure 2(a). This allows for unique optical characterization of each polymer. When large strains are applied to the films, the absorbance of linear polarized light parallel to the strain direction increases relative to the absorbance of polarized light perpendicular to the strain direction over both the spectral range associated with P3HT and the range associated with PCDTPT. This dichroism is associated with the alignment of the polymer backbones in the direction of strain.[29] To quantify the alignment of the polymer in the strained film, we calculated the dichroic ratio of the blend films at a wavelength of 550 nm to track P3HT, and at 900 nm to track PCDTPT, provided in Figure 2(c). We find that the dichroic ratio increases with applied strain and behaves similar with strain at both wavelengths. At a strain of 75%, the dichroic ratio of 2.4 and 2.3 were found at 550 nm and 900 nm, respectively. When the 75% strained film was reduced to lower strains, the dichroic ratio drops following the same trend as found in the tensile strain direction. The film strained by 75% and then reduced to 10% strain has a dichroic ratio of approximately 1.1 at both 550 nm and 900 nm. To determine if this morphology change is consistent over many strain cycles, the films were

repeatedly strained to 75% and then back to 10% for up to 100 cycles with the dichroic ratio measured at these strain limits. As shown in Figure 2(d), the dichroic ratio at 550 nm and 900 nm consistently repeat during the cyclic strain process. These results suggest that when the large tensile strain applied to the film is released, the polymer in the film plastically deform back towards an in-plane isotropic distribution. It is important to note that the absorbance measures the average in-plane orientation of the polymers such that an isotropic backbone distribution and a biaxial orientation distribution will both have a dichroic ratio of 1. It has previously been shown that a P3HT film uniaxially strained in tension by 100% and then strained again in tension in the transverse direction by 100% results in films with a broad crystalline orientation distribution.[30] It is expected that a similar morphological change will occur here, and that when the strain is lowered the polymer backbones will go back toward an in-plane isotropic distribution.

The absorbance can also provide information on the local order of the polymer in the film.[31] To compare how the absorbance features change over many strain cycles, we plot the normalized absorbance for films strained by 75% the 1st time and after 100 cycles, and films strain released back to 10% the 1st time and after 100 cycles in Figure 2(b). We find that the absorbance features are remarkably similar before and after the cyclic strain process. The vibronic features in the P3HT remain almost identical, indicative of similar aggregate order.[31] This is consistent with previous work on strain oriented neat P3HT films where it has been shown that the P3HT orients in the direction of strain without a significant difference in aggregate percentage or aggregate quality.[32] The PCDTPT absorbance is also very similar after the 1st strain cycle and 100th cycle indicative of similar PCDTPT aggregate order.

The change in morphology under cyclic strain was also characterized by grazing incidence X-ray diffraction (GIXD). 2-D GIXD images were taken on films under various number of strain cycles at both 75% strain and at 10% strain, with images shown in Figure 3, and Figure S1. Previously it has been shown that P3HT and PCDTPT crystallites are present in the blend film, and that due to the packing differences of the crystals, their diffraction peaks in the π-stacking and alkyl-stacking directions are separated in reciprocal space.[25] We observe that as the film was strained the diffraction pattern becomes anisotropic with an increase in in-plane diffraction intensity of (100) and (010) peaks when the X-ray beam is parallel to the strain direction (i.e. scattering vector nominally perpendicular to the strain direction). This difference is most clearly observed in the in-plane (100) peaks as indicated in Figure 3. This is indicative of alignment of both the P3HT and PCDTPT crystals with the backbone orienting in the direction of strain. When the strain was released, the diffraction anisotropy decreases, with the in-plane (100) diffraction peaks becoming closer in relative intensity, suggesting that the polymer goes back towards an in-plane isotropic distribution, in agreement with the absorbance anisotropy. Importantly, the diffraction characteristics at a given strain state remain very consistent with increasing strain cycles. In-plane line scans from the 2D images for films in the 1st strain cycle and after 100 strain cycles are provided in Figure S2 to highlight the diffraction similarity. These results provide further support that the cyclic deformation process does not significantly change the local order of both polymers in the blend film, including the crystallinity or crystal size.

The morphology of the strained films was further investigated using atomic force microscopy (AFM), optical microscopy, and scanning electron microscopy (SEM) with results given in Figure 4, Figure 5, and Figure S3. The blend film exhibits some obvious topography changes under large applied strain and strain release. Before being strained, the topography of the film was smooth with an RMS roughness of 1.6 nm. After being strained by 75% there was a significant increase in roughness resulting in an RMS roughness of 5.1 nm. The increased roughness is attributed to inhomogeneous deformation in the film, resulting in features that appear as partial tears. An AFM line scan that compares the substrate height to the film height, given in Figure 4(j), shows that these features are not through the film thickness, and the film remains continuous. When the strained film was released to 10% strain relative to its initial length, the partial tearing features appear to close, and the film RMS roughness reduces to 3.9 nm. Under cyclic strain, we find that at a low number of cycles, the topography of the films is repeated at high and low applied strains. As the number of strain cycles increases we begin to observe large protrusions in the AFM images for films at the 10% strain state, which is attributed to localized delamination of the film. Here, the AFM images are for films transfer printed from PDMS to a Si substrate. The delamination of the film is also observed while on PDMS in the optical microscope images (Figure 5) and SEM images (Figure S3). Comparing the AFM images to the optical microscope and SEM images show that the delamination features are similar before and after the transfer-printing step. It is important to note that the chosen strain range represents a limiting case, and increasing the lower strain limit reduces the observed delamination behavior.

As a comparison to the blend films, neat P3HT films were also cyclically strained. Importantly, there are various reports in the literature regarding the crack onset strain of P3HT films, which can vary from 10%[19] to over 150%[29]. The crack onset depends on a number of factors including the molecular weight of the polymer and the source. The neat P3HT used in this study has a crack onset strain of over 150%. Similar to the blend film, the P3HT plastically deforms under strain, and the dichroic ratio increases with applied strain.[29] Unlike the strained blend film, the film roughness remains similar when strained, and no cracks or partial fracture is present.[29, 32] Upon strain release from the 75% strain limit, significant delamination of the film occurs. Subsequent strain cycles results in severe delamination, which was observed by optical microscopy in Figure 5, and scanning electron microscopy (SEM) in Figure S3. The delamination in the P3HT film is found to be significantly greater than what was found for the blend films and prevented successful transfer printing onto a secondary substrate after the cyclic strain process. The delamination of the P3HT film is consistent with previous work on PEDOT:PSS films where buckling and delamination was observed when large tensile strain applied to ductile films while on an elastomer host was reduced.[22]

During strain reduction, the thin film may buckle out of plane, delaminate, or plastically deform, which depends on the film elasticity, plasticity, and adhesion to the elastomer substrate.[33] The dramatic difference in the cyclic strain character between the blend film and the neat P3HT film is attributed to inhomogeneous elongation that occurs in the film, and a local change in elasticity. Blending the brittle PCDTPT with P3HT results in a blend film that is nominally not as ductile as the neat P3HT film. This is evidenced by the large

increase in film roughness associated with partial tearing observed in the highly strained blend films. Interestingly, the roughness reduces upon strain release suggesting that these localized regions may have a greater plasticity undergoing greater deformation and providing a region of stress relief. The localized thin regions that forms during the strain process is not likely to be only one polymer type given that both the PCDTPT and P3HT are shown to orient during the strain process by a similar magnitude. Spin casting a blend consisting of two immiscible polymers has previously been shown to first form a vertical segregation profile followed by a lateral instability and the formation of large lateral segregated domains of the two polymers.[34] The drying kinetics can limit this evolution in the film formation process. Here, we believe that lateral segregation begins to occur in the film, however solidification arrests the segregation process prior to the formation of pure lateral domains, as previously observed in the 1:1 PCDPTPT:P3HT blend films.[34] This lateral segregation of the polymers in the blend then contributes to the lateral thickness variation with large applied strain. Previously we have shown that the elastic modulus of P3HT lowers upon large applied strain.[35] This drop in modulus will reduce the elasticity mismatch between the film and substrate reducing the driving force for film buckling to occur.[33] In addition, as the film is strained, these localized thin regions may have increased compliance and plasticity associated with thin film confinement effects.[36] In contrast, the neat P3HT film does not have a significant change in roughness with tensile strain, such that a localized change in plasticity may not be present. This may contribute to the P3HT film favoring delamination over plastic deformation during strain release. The adhesion of the film to the elastomer substrate may also play a role in the difference in delamination behavior between the blend film and the neat P3HT film. However, during the transfer printing process, both neat PCDTPT and P3HT films are easily transferred off the PDMS stamp onto a secondary receiving substrate. The secondary receiving substrate includes low surface energy OTS treated silicon, suggesting that both polymers are not strongly adhered to the PDMS. While difference in adhesion between PCDTPT and P3HT may be present, it does not appear to be a primary driving force for the observed delamination behavior.

2.3. OTFT performance

The ability of the blend film semiconductor to function in a stretchable transistor was tested by cyclically straining the films while on a PDMS host substrate, and then transferring printing the films to a rigid bottom gate bottom contact OTFT test bed for device characterization, as illustrated in Figure 1(c). This approach has been applied in a number of studies of stretchable semiconductors given the simplicity of the approach and ability to focus on the semiconductor layer.[13, 16, 18, 29, 37] Once the film was printed, the saturated field effect charge mobility was measured without further processing. The unstrained blend film had a charge mobility of 0.09 +/- 0.01 $cm^2V^{-1}s^{-1}$ for a 5-μm channel length device. The charge mobility channel length dependence is given in Figure S4, showing a drop in mobility with increasing channel length, consistent with low contact resistance behavior.[30] A corresponding neat P3HT film had a charge mobility of 0.04 +/- 0.01 $cm^2V^{-1}s^{-1}$, and a neat PCDTPT film had a charge mobility of 0.10 +/- 0.01 $cm^2V^{-1}s^{-1}$. The charge mobility of the blend film suggests that charge is primarily transporting through the PCDTPT. It is important to note that PCDTPT and P3HT have a similar HOMO energy level such that it is possible that charge may transport through both polymers. The measured charge mobility is

lower than previously reported for PCDTPT, and PCDTPT:P3HT blend films due to the lack of a thermal annealing step after spin casting the films.[24, 28] It was found that when thermally annealing the film immediately after spin casting at 200°C for 10 minutes during initial film processing that once the film is strained the charge mobility lowers to a value similar to the film with no thermal annealing, as shown in Figure S4. When large tensile strain was applied to the films, the charge mobility increases along the direction of polymer alignment and decreases in the transverse direction, as given in Figure S5.[24] For charge transport in the direction of strain, the charge mobility of the blend film increases to 0.16 $cm^2V^{-1}s^{-1}$ at 75% strain. Once the strain was released back to 10% strain, the charge mobility decreases and was found to be 0.08 $cm^2V^{-1}s^{-1}$. For charge transport perpendicular to the strain direction, the charge mobility decreases to 0.04 $cm^2V^{-1}s^{-1}$ at 75% strain, and increases back to 0.1 $cm^2V^{-1}s^{-1}$ upon strain release to 10% strain. The change in charge mobility with strain and strain release is consistent with the changing alignment of the polymers in the film.[29, 38]

The blend films were further strained between 75% and 10% strain for up to 100 cycles to examine the film's electrical stability, with charge mobility for 5 μm channel length devices shown in Figure 6. The other important transistor characteristics including threshold voltage, subthreshold swing and on-off ratio are also plotted with strain cycle in Figure S6 showing relatively stable behavior. The current-voltage curves for a film cyclically strained once and after 100 times are also given in Figure S7 showing very similar characteristics. At the 75% strain limit, the charge mobility remains consistent for charge transport parallel and perpendicular to the strain direction. At the 10% strain limit, the charge mobility drops slightly with increasing number of cycles for charge transport both parallel and perpendicular to the strain direction. The drop in mobility is likely associated with the film delamination at this strain state that increases with cyclic strain. The films are being transfer printed by lamination onto the transistor test structure, where any delaminated film may find improved contact on the receiving substrate. Thus, the impact of delamination may not be fully captured with this measurement approach. However, film distortion near the delamination area occurs during the transfer printing process, as observed by AFM, which likely increasing the resistance to charge transport. The cyclic behavior for 100 μm channel length devices is given in Figure S8 showing similar behavior with strain cycle and transport direction. While there was a drop in charge mobility with strain cycle when the film is held at its lower strain limit, the change is relatively small, particularly compared with changes observed in previous approaches such as semiconductor fibril - elastomer composites.[15, 17] The OTFT results reported here are compared to recent demonstrations in the literature of stretchable organic semiconductors using a similar testing method in Table 1. The comparison includes demonstrations based on block co-polymers,[13] cross-linked polymer semiconductor,[15] crack network films,[37] and fibril-elastomer composite approaches.[16, 18] As shown in Table 1, the findings reported here represent the highest combination of charge mobility and strain-range reported to date.

3. Conclusion

Blending polymer semiconductors has been shown to be a highly effective approach to achieve intrinsically stretchable semiconductors. The PCDTPT:P3HT blend demonstrated

here was previously shown to have vertical segregation of PCDTPT towards the interface with the gate dielectric in an OTFT resulting in charge mobility similar to the neat PCDTPT films. While charge transport is maintained, the ductile P3HT is mixed throughout the film imparting significant plasticity. Under large tensile strain, both polymers are found to orient in the direction of strain, and upon strain release, the compressive force results in a morphology consistent with polymer chains reorienting back towards an in-plane isotropic distribution. During this process, the local order of the polymer was shown to be remarkably consistent. There does appear to be local material inhomogeneity in the film that results in an increase in film roughness with large applied strain. This turned out to be quite advantageous, as it provides locations of stress release during the compression of the elongated film back towards its original shape. The film showed no signs of fracture for strains up to 75% and for 100 strain cycles between 10% and 75% strain. However, as large strain cycles were applied film delamination began to occur at the lower 10% strain limit. When the cyclically strained film was applied in an OTFT, charge mobility was found to track with the polymer alignment. At a given strain state, the charge mobility was found to be consistent up to the 100 applied strain cycles considered in this study; this includes charge mobility consistently above 0.15 $cm^2V^{-1}s^{-1}$ for charge transport parallel to the strain direction at the 75% strain limit. This approach is the first report to achieve an intrinsically stretchable polymer semiconductor film where the film is comprised solely of semiconductor material. In conclusion, polymer semiconductor blends is a promising and facile method to achieve intrinsically stretchable organic semiconductor films.

4. Experimental Section

Film Processing

The blend film was cast from a 4:6 weight ratio of PCDTPT:P3HT dissolved in a 1:1 volume ratio of 1,2-dichlsorobenzene:chloroform. The PCDTPT was synthesized following a previously described process,[28] and had a number average molecular weight of 71 kg/mol, and a polydispersity of 4.9. The regioregular P3HT was obtained from Sigma-Aldrich, Inc., with a number average molecular weight Mn = 54 kg/mol, a polydispersity of 2.4.[39] The solution was spun cast onto OTS treated Si substrate at 1500(2π) rad/min (1500 rpm) for 30 s at room temperature. The films were then transferred onto a PDMS slab mounted on a custom-made strain stage for subsequent straining and morphological characterization. The strain process was done by hand and the strain rate varied but was at most 10%/s. The polymer semiconductor films were transferred again to the final receiving substrate for transistor fabrication, X-ray diffraction measurements, and AFM measurements. Cyclic strain was done in a nitrogen atmosphere and transfer printing was conductive in ambient air. The transfer-printing technique is described in detail in previous work.[30] The PDMS was Slygard 184 and was prepared at a 10:1 base to cross-linking ratio and cured in a vacuum oven held at approximately 85 kPa at 60°C over a period of approximately 12 hours.

Morphology characterization

UV-visible spectroscopy measurements were made using an Ocean Optics Jazz spectrometer. The absorbance of the films were measured while on a PDMS substrate and measured at multiple strain states. The AFM images were measured using an Asylum

MFP-3D-BIO in tapping mode. The X-ray diffraction measurements were made at the Stanford Synchrotron Radiation Lightsource (SSRL) on beamline 11-3 with an area detector (Rayonix mar CCD225), an energy of 12.735 keV, and an incidence angle of ≈0.12°. The SEM images were measured using FEI Verios 460L field-emission scanning electron microscope. The films were measured while on a PDMS substrate and coated with 10 nm of Au to remove charging effects.

OTFT characterization

After straining the film-PDMS stack by a specified amount, the films were transferred printed onto bottom gate, bottom contact OTFT test beds. The source-drain electrodes consisted of a 5 nm Ti wetting layer, followed by 40 nm of Au. The channel length was 5 μm and the channel width was 1000 μm. The gate dielectric was an OTS treated SiO_2 layer that was 300 nm thick. The highly doped Si wafer formed the gate electrode. Charge mobility was measured in the saturation regime with a source-drain voltage of -60 V, and sweeping the gate voltage from 25 V to -60 V, with typical results shown in Figure S5. The charge mobility was determined by taking the slope of the square root of current versus gate voltage over a minimum 5 V range.

Supplementary Material

Refer to Web version on PubMed Central for supplementary material.

Acknowledgments

This research work was supported by the National Science Foundation award CMMI-1554322, and by the NCSU RISF program. Research at UCSB for the synthesis of PCDTPT was supported through the Mitsubishi Chemical Center for Advanced Materials (MC-CAM). X-ray diffraction was carried out at the Stanford Synchrotron Radiation Lightsource, a national user facility operated by Stanford University on behalf of the U.S. Department of Energy, Office of Basic Energy Sciences. SEM measurements were carried out at the Analytical Instrumentation Facility at North Carolina State University.

References

1. Hammock ML, Chortos A, Tee BCK, Tok JBH, Bao ZA. Adv Mater. 2013; 25:5997. [PubMed: 24151185]
2. Kim DH, Lu NS, Ma R, Kim YS, Kim RH, Wang SD, Wu J, Won SM, Tao H, Islam A, Yu KJ, Kim TI, Chowdhury R, Ying M, Xu LZ, Li M, Chung HJ, Keum H, McCormick M, Liu P, Zhang YW, Omenetto FG, Huang YG, Coleman T, Rogers JA. Science. 2011; 333:838. [PubMed: 21836009]
3. Lipomi DJ, Tee BCK, Vosgueritchian M, Bao ZN. Adv Mater. 2011; 23:1771. [PubMed: 21491510]
4. Kaltenbrunner M, White MS, Glowacki ED, Sekitani T, Someya T, Sariciftci NS, Bauer S. Nat Commun. 2012:3.
5. Liang JJ, Li L, Niu XF, Yu ZB, Pei QB. Nat Photonics. 2013; 7:817.
6. Wang JX, Yan CY, Chee KJ, Lee PS. Adv Mater. 2015; 27:2876. [PubMed: 25788429]
7. Park J, Lee Y, Hong J, Ha M, Jung YD, Lim H, Kim SY, Ko H. ACS Nano. 2014; 8:4689. [PubMed: 24592988]
8. Chortos A, Lim J, To JWF, Vosgueritchian M, Dusseault TJ, Kim TH, Hwang S, Bao ZA. Adv Mater. 2014; 26:4253. [PubMed: 24740928]
9. Qiu LZ, Lee WH, Wang XH, Kim JS, Lim JA, Kwak D, Lee S, Cho K. Adv Mater. 2009; 21:1349.
10. Lee Y, Shin M, Thiyagarajan K, Jeong U. Macromolecules. 2016; 49:433.

11. Kim DH, Xiao JL, Song JZ, Huang YG, Rogers JA. Adv Mater. 2010; 22:2108. [PubMed: 20564250]
12. Liang JJ, Li L, Chen D, Hajagos T, Ren Z, Chou SY, Hu W, Pei QB. Nat Commun. 2015:6.
13. Peng R, Pang B, Hu DQ, Chen MJ, Zhang GB, Wang XH, Lu HB, Cho K, Qiu LZ. J Mater Chem C. 2015; 3:3599.
14. Young, RJ., Lovell, PA. Introduction to Polymers. 3rd. CRC Press; Boca Raton, FL, USA: 2011.
15. Wang GN, Shaw L, Xu J, Kurosawa T, Schroeder BC, Oh JY, Benight SJ, Bao Z. Adv Funct Mater. 2016; 26:7254.
16. Shin M, Oh JY, Byun KE, Lee YJ, Kim B, Baik HK, Park JJ, Jeong U. Adv Mater. 2015; 27:1255. [PubMed: 25581228]
17. Choi D, Kim H, Persson N, Chu PH, Chang M, Kang JH, Graham S, Reichmanis E. Chem Mater. 2016; 28:1196.
18. Song E, Kang B, Choi HH, Sin DH, Lee H, Lee WH, Cho K. Adv Electron Mater. 2016; 2
19. Printz AD, Savagatrup S, Burke DJ, Purdy TN, Lipomi DJ. RSC Adv. 2014; 4:13635.
20. Savagatrup S, Printz AD, O'Connor TF, Zaretski AV, Lipomi DJ. Chem Mater. 2014; 26:3028.
21. Awartani O, Lemanski BI, Ro HW, Richter LJ, DeLongchamp DM, O'Connor BT. Adv Energy Mater. 2013; 3:399.
22. Lipomi DJ, Lee JA, Vosgueritchian M, Tee BCK, Bolander JA, Bao ZA. Chem Mater. 2012; 24:373.
23. Savagatrup S, Chan E, Renteria-Garcia SM, Printz AD, Zaretski AV, O'Connor TF, Rodriquez D, Valle E, Lipomi DJ. Adv Funct Mater. 2015; 25:427.
24. Oh JY, Kim S, Baik HK, Jeong U. Adv Mater. 2016; 28:4455. [PubMed: 26460551]
25. Scott JI, Xue X, Wang M, Kline RJ, Hoffman B, Dougherty D, Zhou C, Bazan GC, O'Connor BT. ACS Appl Mater Inter. 2016; 8:14037.
26. Scaccabarozzi AD, Stingelin N. J Mater Chem A. 2014; 2:10818.
27. Moulton J, Smith P. J Polym Sci, Part B: Polym Phys. 1992; 30:871.
28. Ying L, Hsu BBY, Zhan HM, Welch GC, Zalar P, Perez LA, Kramer EJ, Nguyen TQ, Heeger AJ, Wong WY, Bazan GC. J Am Chem Soc. 2011; 133:18538. [PubMed: 21936564]
29. O'Connor B, Kline RJ, Conrad BR, Richter LJ, Gundlach D, Toney MF, DeLongchamp DM. Adv Funct Mater. 2011; 21:3697.
30. Gargi D, Kline RJ, DeLongchamp DM, Fischer DA, Toney MF, O'Connor BT. J Phys Chem C. 2013; 117:17421.
31. Clark J, Chang JF, Spano FC, Friend RH, Silva C. Appl Phys Lett. 2009:94.
32. O'connor BT, Reid OG, Zhang XR, Kline RJ, Richter LJ, Gundlach DJ, DeLongchamp DM, Toney MF, Kopidakis N, Rumbles G. Adv Funct Mater. 2014; 24:3422.
33. Stafford CM, Harrison C, Beers KL, Karim A, Amis EJ, Vanlandingham MR, Kim HC, Volksen W, Miller RD, Simonyi EE. Nat Mater. 2004; 3:545. [PubMed: 15247909]
34. Heriot SY, Jones RA. Nature Mater. 2005; 4:782. [PubMed: 16142241]
35. Awartani O, Zhao B, Curie T, Kline RJ, Zikry MA, O'Connor BT. Macromolecules. 2016; 49:327.
36. Stafford CM, Vogt BD, Harrison C, Julthongpiput D, Huang R. Macromolecules. 2006; 39:5095.
37. Wu HC, Benight SJ, Chortos A, Lee WY, Mei JG, To JWF, Lu CE, He MQ, Tok JBH, Chen WC, Bao ZN. Chem Mater. 2014; 26:4544.
38. Xue X, Chandler G, Zhang XR, Kline RJ, Fei ZP, Heeney M, Diemer PJ, Jurchescu OD, O'Connor BT. ACS Appl Mater Inter. 2015; 7:26726.
39. Certain commercial equipment, or materials are identified in this paper in order to specify the experimental procedure adequately. Such identification is not intended to imply recommendation or endorsement by the National Institute of Standards and Technology, nor is it intended to imply that the materials or equipment identified are necessarily the best available for the purpose.

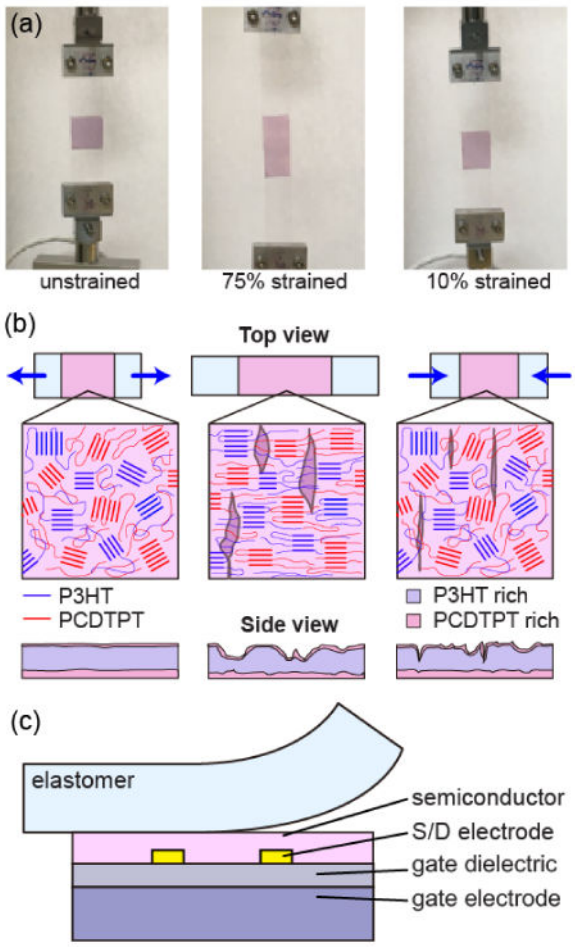

Figure 1.

(a) Photos of an unstrained film, 75% strained film and strain-released film at 10% strain while on PDMS. (b) Illustration of the change in film morphology during the cyclic strain process from a top view and side view. At large tensile strain, the illustration includes alignment of both polymers and partial tearing features. When the strain is reduced the polymer alignment reduces and tearing features narrow. The side view includes an illustration of the vertical segregation of the polymers found in the blend film. (c) An illustration of transfer printing the polymer semiconductor film from the elastomer stamp to an OTFT test bed.

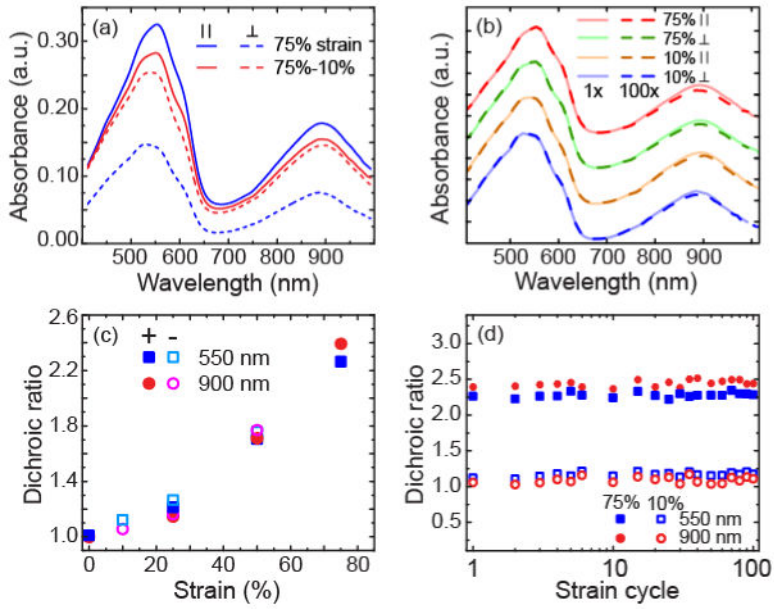

Figure 2.

(a) Absorbance of the PCDTPT:P3HT blend film at 75% strain and film strained to 75% and then lowered to 10% under polarized light parallel (∥) and perpendicular (⊥) to the strain direction. (b) The normalized absorbance of the blend film at 75% strain and at 10% strain, comparing the first strain cycle (1×) to 100 cycles (100×). The measured absorbance at a specific strain state and polarized light orientation are normalized and offset for clarity. The absorbance at a specified strain state and light polarization during the first strain cycle and after 100 cycles are plotted together to compare absorbance features. (c) The dichroic ratio of the blend film under tensile strain (+) and reduction of the applied strain (-) during the first strain cycle. The dichroic ratio is taken at 550 nm and at 900 nm to capture the P3HT and PCDTPT, respectively. (d) The dichroic ratio of the blend film at 75% strain and 10% strain with increasing number of strain cycles.

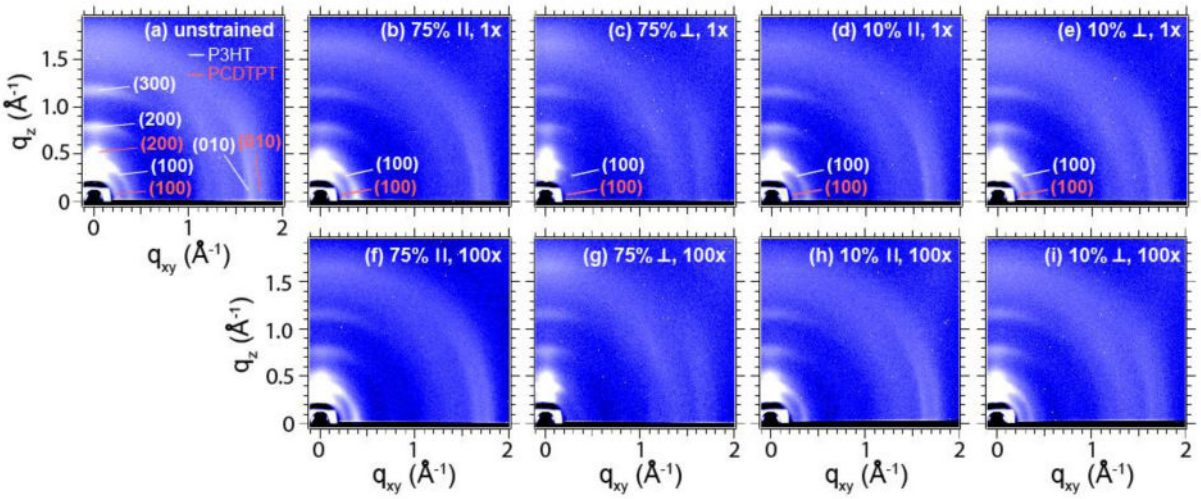

Figure 3.

Two dimensional grazing incidence X-ray diffraction images of (a) an unstrained film, and strained films during the (b-e) first strain cycle and after (f-i) 100 strain cycles held at 75% strain and 10% strain as specified. The X-ray beam is incident parallel (∥) or perpendicular (⊥) to the strain direction as labeled.

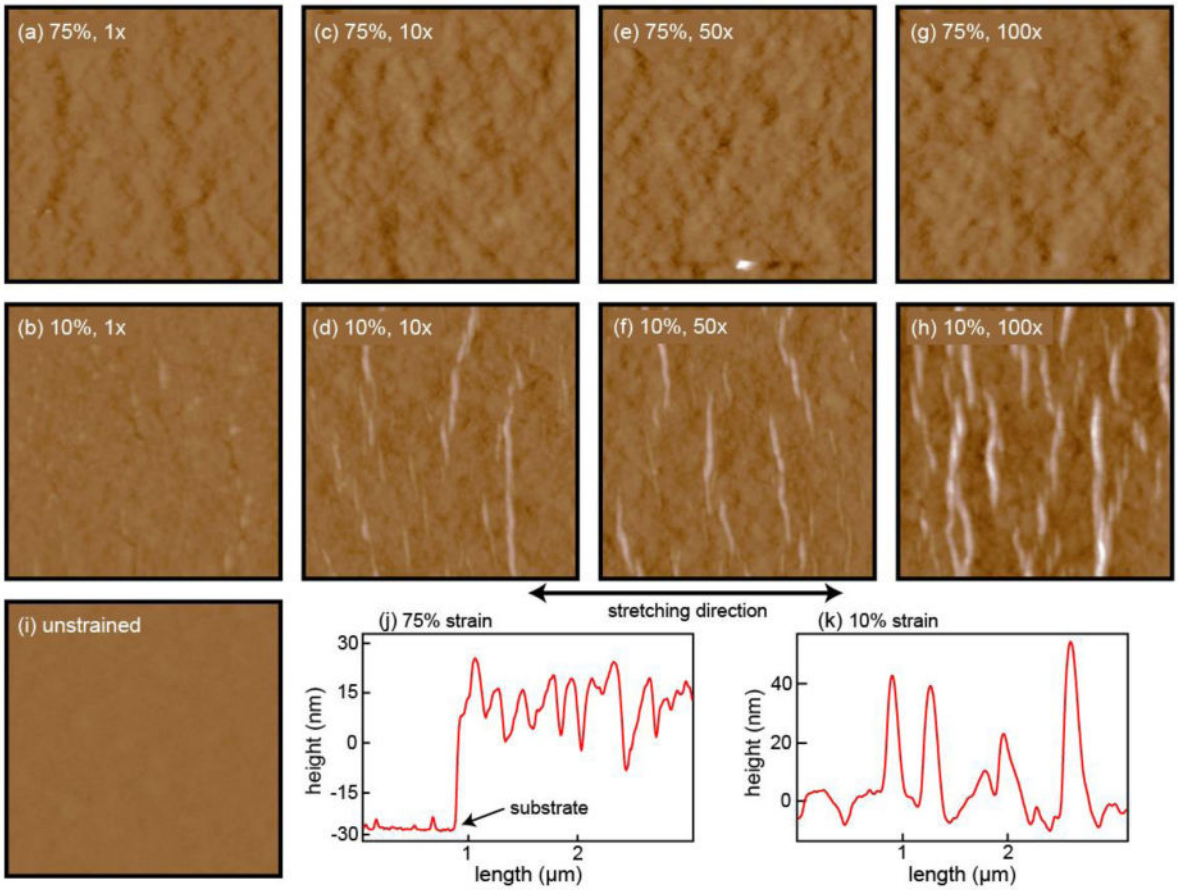

Figure 4.

AFM height images of films strain by 75% and then lowered to 10% strain after (a,b) 1, (c,d) 10, (e,f) 50 and (g,h) 100 strain cycles. (i) An AFM image of an unstrained film. The area of all images are 5 μm × 5 μm. The black arrow shown below the AFM images provides the direction the film was strained. Line scans for films at (j) 75% strain and (k) 10% strain after 100 strain cycles. The line scan for the 75% strained film is given at the edge of the film to show that the roughness is not through the film thickness.

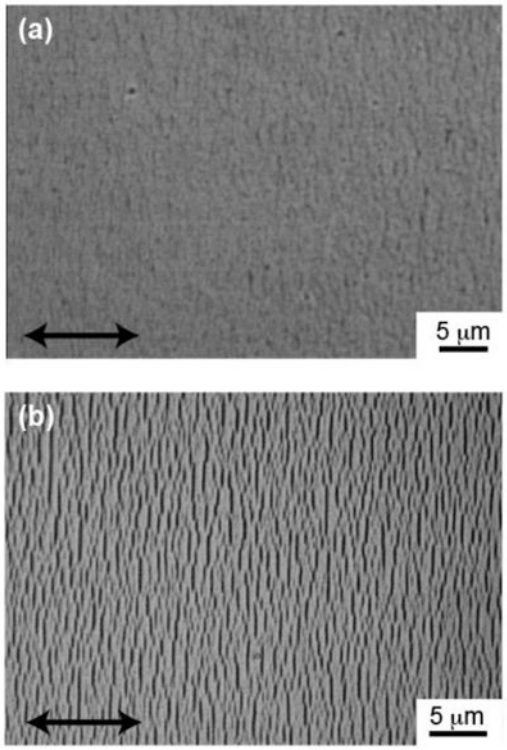

Figure 5.

Optical microscope image of (a) a PCDTPT:P3HT blend film at 10% strain after 50 strain cycles, and (b) a P3HT film at 10% strain after 10 strain cycles between 75% strain and 10% strain. Arrows in figure indicate the applied strain direction. Both images are taken while on the PDMS substrate. Clear differences in delamination (dark lines) are observed between films.

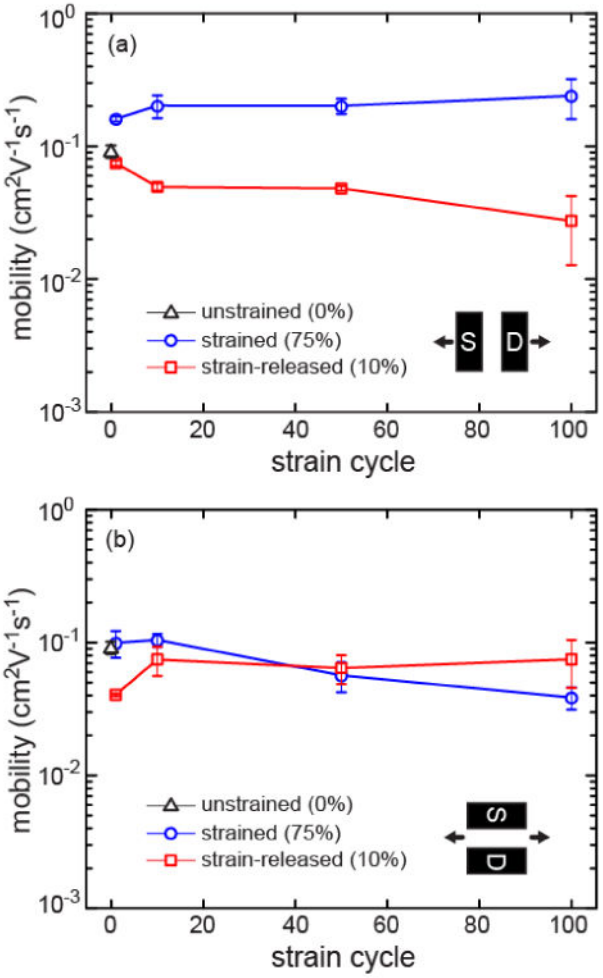

Figure 6.

Saturated field effect mobility for (a) charge transport parallel to the strain direction, and (b) charge transport perpendicular to the strain direction for films at 75% strain and films released to 10% strain for a specified number of strain cycles. Charge mobility is also reported for an unstrained film. The channel length for the transistors is 5 μm.

Table 1

A comparison of OTFT characteristics of stretchable organic semiconductors tested on rigid test-beds after cyclic strain. The reported range in charge mobility is for 100 strain cycles, except the block copolymer approach, which is for 1 time tensile strain only.

Approach	Mobility ($cm^2V^{-1}s^{-1}$)	On/Off	Strain range (%)	Ref.
Block-copolymer	$<2x10^{-4}$	10^2	60	[13]
Semiconductor fibril-elastomer composite	0.006-0.001	10^5	50	[17]
Semiconductor fibril-elastomer composite	<0.001	10^3	100	[15]
Crack network	0.02-0.008	10^5	15	[37]
Cross-linked DPP	0.4-0.3	--	20	[15]
Polymer blend[a)]	0.04-0.02	10^3	65	*This work*
Polymer blend[b)]	0.25-0.16	10^4	65	*This work*

[a)] Charge transport perpendicular to the strain direction

[b)] Charge transport parallel to the strain direction at 75% strain